Annexure-A

i. Brief Objective of the Project:

The interest in TM oxides is driven by the immense potential of this material as it holds a variety of technological applications. The important technological applications of these metal oxides are in photocatalysis, photochemical solar cells, optoelectronic devices, chemical sensors, and dielectric material of ultrathin thin-film capacitors. However, until now there is no detailed experimental and theoretical evidence of the length scale of disorder nor there is a clear picture of the phase transition in these compounds which are many time exist in amorphous structures, specifically in the case of pressure induced amorphisation in **TM oxides**. **The specific objectives of the proposed project may be classified as follows:**

1. To investigate the ground state optimized geometries and convergence with k-points, choice of pseudopotential for different phases.
2. To investigate (using first principles calculations) the stable structure of dioxides with respect to different physical parameter like pressure, temperature etc.
3. To calculate Electronic band structure, electronic density of states (DOS) and mechanical properties.
4. To calculate full phonon dispersion curve at high symmetry direction and to understand the unresolved issues of the structural details and atomic-scale picture of the high-density amorphous (HAD) phase using first principles calculations.
5. To understand the unusual compression behaviour in anatase with a sharp increase in stiffness around transition pressure.
6. Pressure dependence of the different phase of Raman modes using density functional perturbation teory to understand pressure-induced amorphization (PIA).
7. Raman tensor and pressure dependent Raman spectra of the metal oxides and compare with available results.
8. To find out the oxygen diffusion in these TM oxides materials and further calculate spin polarized calculation for the system with magnetic ions.

ii. Work done so far and results achived and publications if any resulting from the work

1. Lattice dynamics and Raman spectrum of rutile TiO_2: The role of soft phonon modes in pressure induced phase:

In this work, one of the goals was to carry out density functional perturbation theory (DFPT) calculations in order to investigate the lattice dynamical properties and their variation with pressure to identify soft phonon modes associated with pressure induced structural

instability. It is a known fact that lattice dynamics can reveal important information about the pressure induced phase transitions, especially when lattice dynamical instabilities are involved. Second, intensities of Raman lines are important part of the information contained in the vibrational spectra of crystals. Due to the changes in the crystal structure, as a response to an external perturbation (like pressure or temperature), the frequencies, as well as the intensities of Raman active modes, change under the external influence.

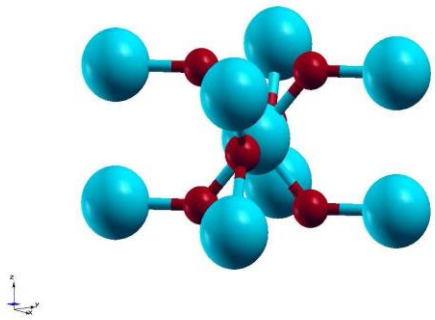

FIG. 1. Schmatic view of the rutile structure in TiO_2. Blue balls represent Ti and red balls O atoms.

At the first stage, the structural optimization of rutile TiO_2 has been performed under the minimum condition of the total energy and the forces acting on atoms, for each pressure needed in the response function calculations. As a result, we obtained the equilibrium values of the lattice constants and internal parameter *u*. The lattice constants obtained in the case of rutile TiO_2 phase (Fig. 1) agree well with experimental and previously reported values, which are presented in Table I. In order to get an idea about the behaviour of phonons and their role played in the stability of structure and phase transformation in rutile TiO_2, we have calculated full phonon dispersion curves (PDC) for rutile TiO_2 phase at zero and higher pressures. The calculated full PDC along major symmetry directions of the Brillouin zone (BZ) at zero and higher pressures are presented in Fig. 2. For the rutile phase, there are 6 atoms in the primitive cell; thus, there should be 15 optical modes and three acoustic modes. From the group analysis of its space group (P42/mnm), the optical modes at the Γ-point belong to the following irreducible representations:

$$\Gamma_{opt} = A1g + A2g + A2u + 2B1u + B1g + B2g + Eg + 3Eu ,$$

Where symbol g represents Raman active, u infrared active and E degenerate modes. In principle, the long-range dipole-dipole interactions in the ionic compounds can result in the LO-TO splitting. The LO-TO splitting occurs at the Γ-point and only for infrared active modes. Since A_{2u} and E_u modes are polar, they split into LO and TO modes with different frequencies due to macroscopic electric fields associated with the LO phonons. A_{2g} and B_{1u} modes, however, are Raman and infrared inactive (silent modes). Fig. 2 reveals that the all phonon modes are positive in the phonon dispersion curves of rutile TiO_2 at ambient pressure, while the PDC at high pressure contain an unstable phonon mode at Γ- point and a slightly soft mode at A point, which eventually becomes unstable at even higher pressures (around 20 GPa). This reflects and confirms that the rutile at ambient pressure is a dynamically stable structure. A closer inspection of the PDC would reveal that the lattice dynamical instability begins at the pressure of 5GPa. The presence of imaginary frequencies in the phonon dispersion curves of rutile phase of TiO_2 at the pressure bellow 10 GPa (Fig. 2(c)) supports the dynamical instability and leads to another structure (columbite).

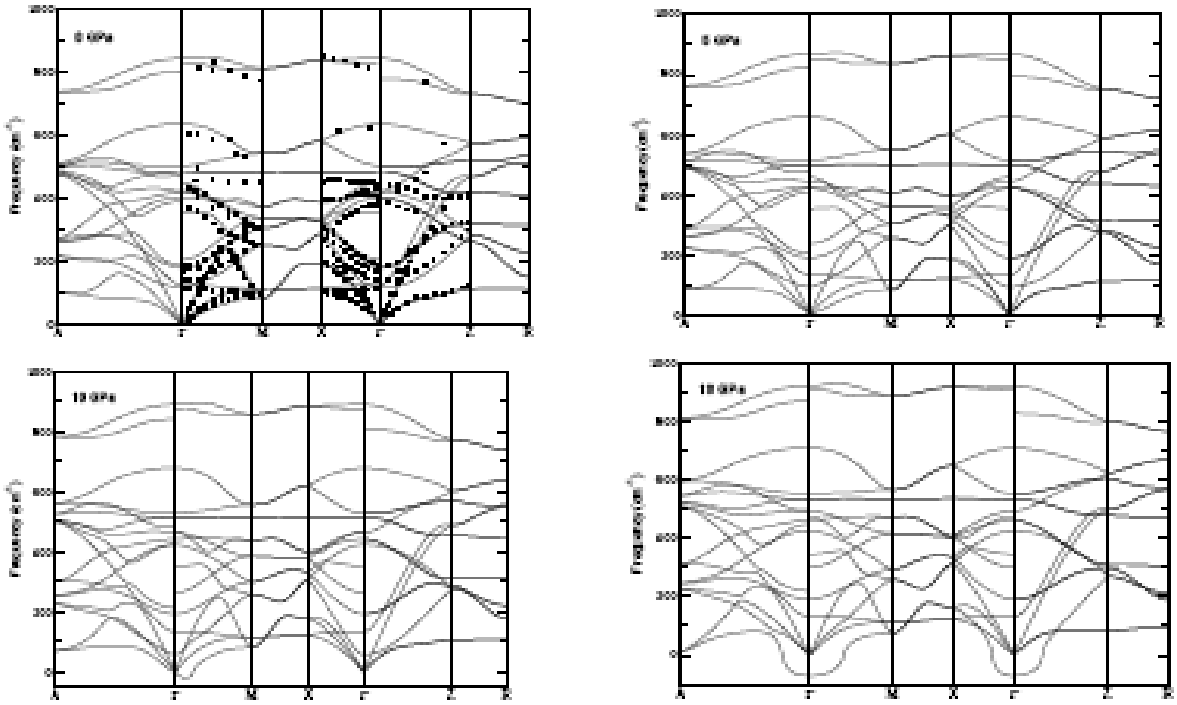

FIG. 2. Phonon dispersion curves at four different pressures: 0 GPa, 5 GPa, 10 GPa and 18 GPa.

The lattice dynamical instability at Γ- point is seen already at 10 GPa, while at 18 GPa a clear instability occurs. Squares represent the experimental results for comparison. Furthermore, we should note that there are few states in the region above 600 cm^{-1}. It is also seen from the Fig. 2 that less difference in mass between anions and cations results in a lesser gap and hence the divergence (~280 cm^{-1}) between the acoustic and optical phonon branches.

A much better understanding of the high pressure behaviour of the PDC can be obtained using the mode Gr¨uneisen parameters. Mode Gr¨uneisen parameters for all modes and along the high symmetry directions (as in PDC) are shown in Fig. 3. The parameters for the Raman active modes agree reasonably well with the experimentally determined ones of Samara and Peercy: for B_{1g}, E_g and A_{1g} modes we got the values -12.96, 1.54 and 1.83, while Samara and Peercy got -5.03, 2.43 and 1.59, respectively.

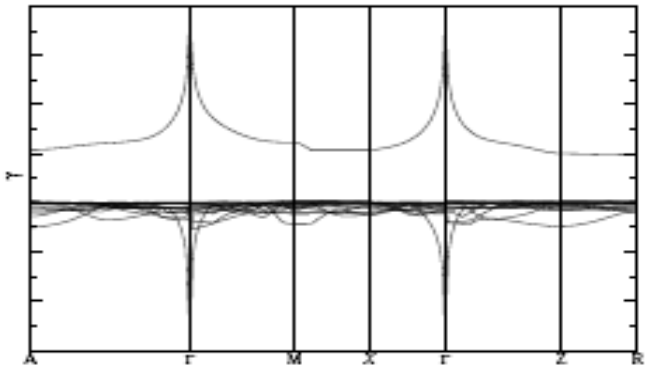

FIG. 3. Mode Gr¨uneisen parameters in the rutile phase of TiO_2, showing the pressure trends for all the modes and along the high symmetry directions in the Brillouin zone.

The discrepancies between our calculated and experimentally measured values probably arise because the pressure interval in which Samara and Peercy measured the phonon frequencies is much narrower (up to 0.35 GPa) than the one we used (5 GPa), although this reasoning cannot be applied to the B_{1g} mode, since the shift of its frequency is

almost linear with pressure. A large negative parameter is clearly seen for the transversal acoustic mode at the Γ-point, which causes the lattice dynamical instability in the rutile phase. The positive parameters are present for the high energy phonon branches through the whole Brillouin zone, especially at the Γ-point, explaining their hardening with increasing pressure. Larger negative parameters are also present at the A, M and Z points. Supposable, this negative trend will continue even further, with increasing pressure, at the A point for the transversal acoustic mode, and drive it toward the instability at pressures around 20 GPa, as commented above. The rest of the modes have mild negative parameters.

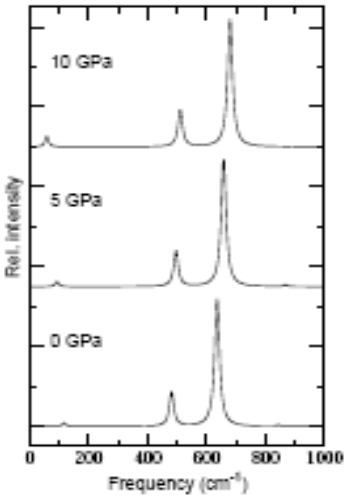

FIG. 4. Raman spectra in the rutile phase of TiO_2 at 0, 5 and 10 GPa. No significant changes in the intensities of the Raman lines can be observed.

The Raman spectrum of rutile TiO_2 at the pressures of 0, 5 and 10 GPa is observed in the present research and shown in Fig. 4, where all four Raman peaks theoretically expected appear distinctly. Raman line intensities at zero pressure, on the other hand, cannot be easiliy compared to the experimental line intensities. Only a qualitative comparison can be given with the spectrum. Our calculations properly reproduce which Raman mode has the largest intensity, which one the second largest, and so on. The intensities ratios, however, show greater discrepancy: for example, I_{Eg}/I_{B1g} is about 3.2 in experiments, while our calculations give the ratio of 12. Some justifications for these two results can be sought in the facts that intensities measured during the Raman experiments depend on many external variables (especially when conducting the spectroscopy under pressure using diamond anvil cells), like the shape or the quality of the material sample, and that our calculated intensities are for the completely powdered sample, while it may not be so in real experiment. For the current research, a more important feature is the pressure dependence of the Raman line intensities, calculated from the components of the Raman tensor. Although, there are numerous cases in which pressure induces significant changes in the intensities of the Raman lines, we find that there are no such changes in the case of rutile TiO_2: all the TiO_2 rutile modes' intensities change very little in the pressure region from 0 to 10GPa. A comparison with the high pressure Raman spectra (at 10.4 GPa) reveals that the mode (around 450 cm^{-1}) with increased intensity is actually not the Eg mode of the rutile phase, but belonging to the one of the Raman active modes of the higher pressure phase of TiO_2 -columbite. This also points to the fact that columbite phase begins to occur at the pressure below 10 GPa.

2. A First Principles Lattice Dynamics and Raman Spectra of the Ferroelastic Rutile to $CaCl_2$ Phase Transition in SnO_2 at High Pressure

Over the past of few years attention has been focused on the research field of metal/semiconductor oxide bulk and nano materials such as highly crystalline SnO_2, TiO_2, RuO_2, and CrO_2 because of their fundamental importance and the wide range of their potential applications in nanodevices. Semiconducting nanostructural materials are known to have many interesting physical properties and great applications in optoelectronic devices, solar energy conversion, nonlinear optical, photoelectrochemical cells and heterogeneous catalysis. However, RuO_2 have received a lot of attention mostly based on their importance for applications in electrochemistry catalysis and ferroelectric random access memories]. Especially RuO_2 has been studied in great details to understand the mechanism for the catalytic carbon monoxide oxidation on RuO_2 (110) surface. Density functional calculations have been applied to these systems quite successfully; however, detailed understanding of the above mention phenomena requires a proper treatment of temperature and pressure. The concept for dealing with these complications is known as abinitio thermodynamics. In order to understand proper lattice dynamical behavior and its pressure dependence we first calculated the equilibrium lattice parameter by calculating the total energy enthalpy obtained for different volumes. The equilibrium lattice parameters so obtained are in good agreement with previous experimental and theoretical findings The Birch–Murnaghan third order equation employed to calculate the equilibrium volume V, bulk modulus B, first order pressure derivative of bulk modulus B' and lattice parameter for SnO2. There is very good agreement between experiment and other theoretical results. A unit cell of tetragonal phase of SnO2 is shown in Fig. 6. It is consist of 2 Si and 4 Oxygen atoms.

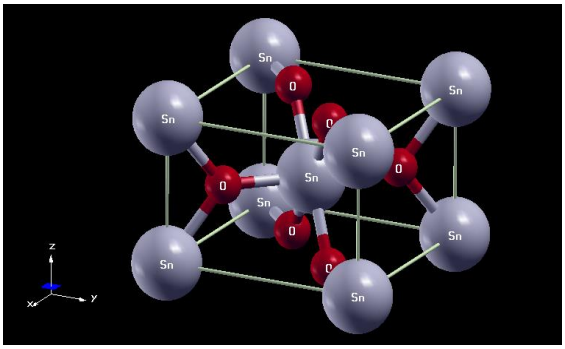

FIG. 5. Schematic view of the rutile structure in SnO_2. Blue balls represent Sn and red balls O atoms.

To investigate the changes that occur in the phonon spectrum of tetrahedral and octahedral crystal of SnO_2 at high pressure, we have calculated the phonon dispersion curves along with phonon density of states up to 20GPa using first principles calculations within the framework of density functional theory. It is an established fact that the B_{1g} Raman active mode frequency shows characteristic behavior and decreases with increasing pressure, contrary to the typical behavior observed for other Raman active modes in the case of retile SnO_2 similar to other isostrcutural rutile dioxides. This softening of the B_{1g} Raman mode indicates a strcuctural instability which is the precursor of phase transition. The results obtained from the first principles calculations were analysed using group theoretical arguments and the landau theory of phase transition.

To assess the behaviour all frequencies at the zone centre, the pressure dependence all zone centre phonon modes analyzed. According to group theory the rutile structure has following phonon modes at centre of Brillouin zone.

$$\Gamma = 2A_{2u}(IR) + 4E_u(IR) + B_{1g}(R) + 2B_{1u} + A_{2g} + E_g(R) + A_{1g}(R) + B_{2g}(R) \quad (9)$$

Where R and IR corresponds to Raman and infrared active mode, The simulated LDA and GGA phonon frequencies for all modes are in agreement along with previous theoretical and experimental Raman data. In order to investigate the stability of the rutile SnO_2 crystal structure, we calculated the phonon frequencies for various symmetry directions in the Brillouin zone (BZ). i.e. the phonon dispersion curves (PDC) (Fig. 6) at the pressure close to the transition pressure we found that all phonon frequencies are real at the pressure of few GPa below the transition pressure.

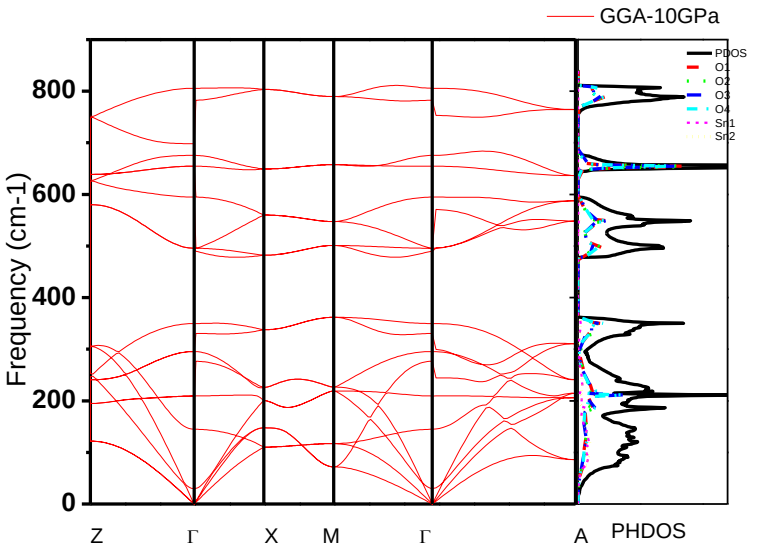

Figure 6. Phonon dispersion curves and phonon density of states of SnO_2 in rutile phase at 10 GPa pressure

The right panel of these dispersion curves represents the corresponding phonon density of states. However, we observed the softening of B_{1g} Raman active mode at zone centre at 10GPa. A close look of the phonon dispersion curves in Fig. 8 depicts that the transverse acoustic phonon branch is imaginary in the vicinity of zone centre arising from the interaction of B_{1g} Raman mode mainly responsible for destabilizing the tetragonal rutile SnO_2. This phase transition pressure of 12GPa is in good agreement to experiment in contrast to previous reported transition pressure obtained from the similar method. The phonon dispersion curves presented at zero pressure is in overall good agreement with earlier calculated phonon dispersion curves and available experimental data. There are however minor differences, with earlier theoretical calculations such as the lack of crossing of $Eu^{(1)}$ mode in Γ-X direction and almost degenerate low lying acoustic modes in X-M direction of the Brillouin zone. The phonon density of states reflects all general features of phonon dispersion curves. The Sn and O atoms vibrations almost equally contribute to the phonon density of states up to 10.5THz, while the major contribution to 12-23THz is due to O atom vibrations. In order to clarify the structural mechanism of the phase transition and to obtain more insights in to the stability of the phases at higher pressures, we have calculated the theoretical Raman and infrared spectra (intensity vs frequency curve) up to 20GPa for rutile SnO_2.

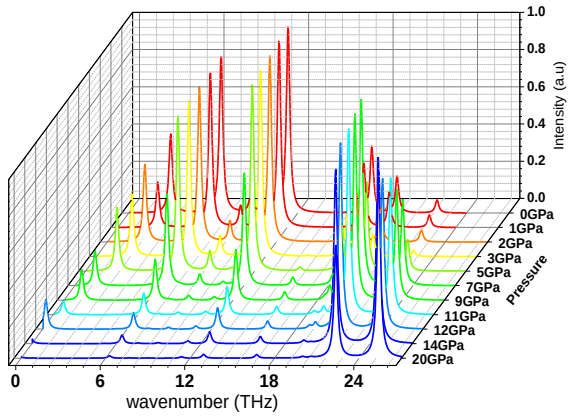

Figure 7. Calculated high pressure onset Raman intensity up to 20 GPa for rutile SnO_2

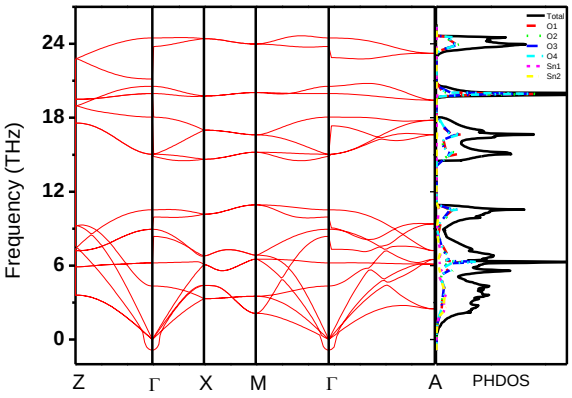

Figure 8. Phonon dispersion curves and phonon density of states of SnO_2 in rutile phase at transition pressure (12GPa).

diminishes along with around 11GPa, the phase transition pressure. However, the frequency of other modes increases as per the normal expectation due to compressed bands under the influence of pressure. For the current research, a more important feature is the pressure dependence of the Raman line intensities calculated from the component of Raman tensor. We find while intensity of several peaks increases, the peak intensity for several peak diminishes at around the phase transition pressure of 12GPa.

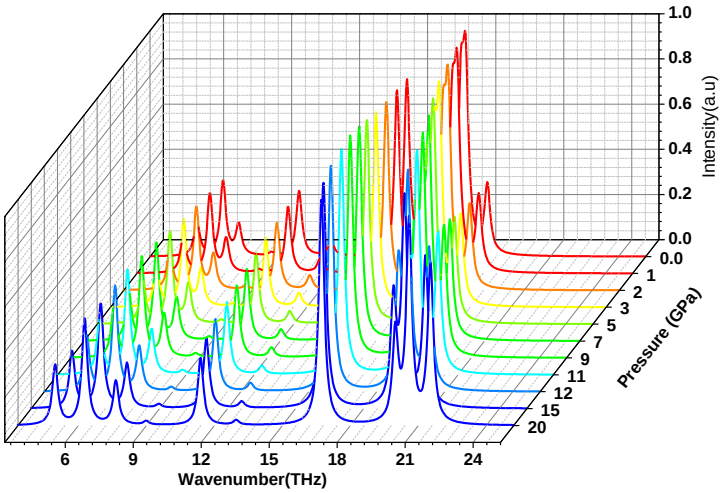

Figure 9. Calculated high pressure onset Infrared spectra up to 20 GPa for rutile SnO_2

These are indicative features of phase transition. To have a clear evolution of peaks and its intensity with pressure, we plot a three dimensional pressure dependent Raman intensity plots. This figure clearly brings out the relative intensity of peaks. We also present the pressure dependent infrared intensity plot of rutile SnO_2 in Fig. 9. These figure do not however show any disappearance of modes, and its intensity which is quite obvious but shows the pressure dependent shift of peak positions. In order to investigate the elastic instability in rutile SnO_2 (stishovite) responsible for the transition, we have optimized tetragonal unit cell at a given pressure by slightly distorting under an orthorhombic strain and reoptimizing the ionic positions in the strained lattice. This methodology has also been used to investigate the phase boundaries of high pressure polymorphs of silica. The calculated

pressure variation of elastic constants of the rutile SnO_2 is plotted in Fig. 10 along with the experimentally derived elastic constants from Brillouin spectroscopy. There is reasonably good agreement between present theory and experiment.

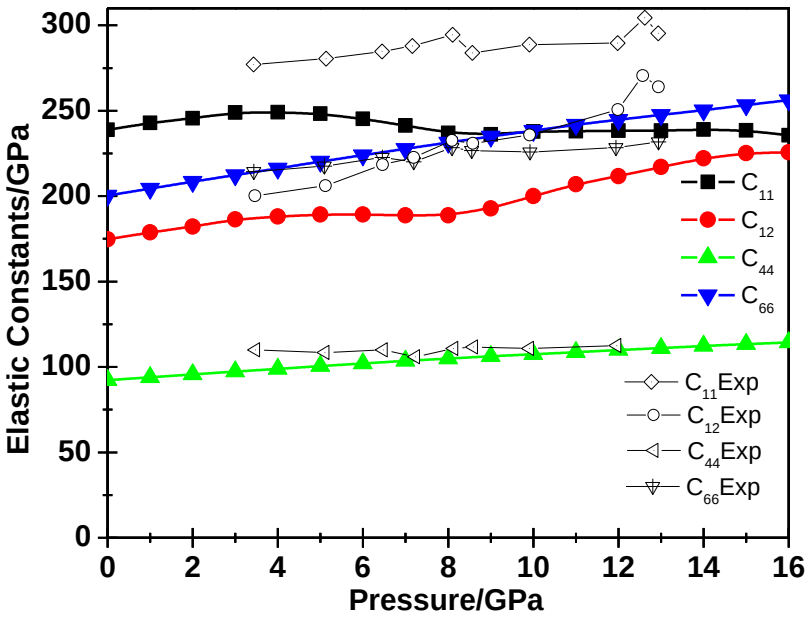

Figure 10. Calculated elastic constants together with the Brillouin spectroscopy data.

Fig. 11 shows the variation of shear of modulus, (C11-C12)/2 which reveals that the shear modulus becomes negative at high pressure with (C11-C12)/2 = 0 at 14.9 GPa, implying that this is transition pressure. This figure also indicates the experimentally obtained shear modulus from and shows a reasonably good agreement in terms of both values and trend. The transition pressure even obtained from the interpolation of Brillouin data (14.6 GPa) is in excellent agreement. This indicates a strongly coupling between Raman modes and elastic constants as we did not found calculated shear modulus to become softer with pressure in the case of ions not allowed to relax in the distorted cell

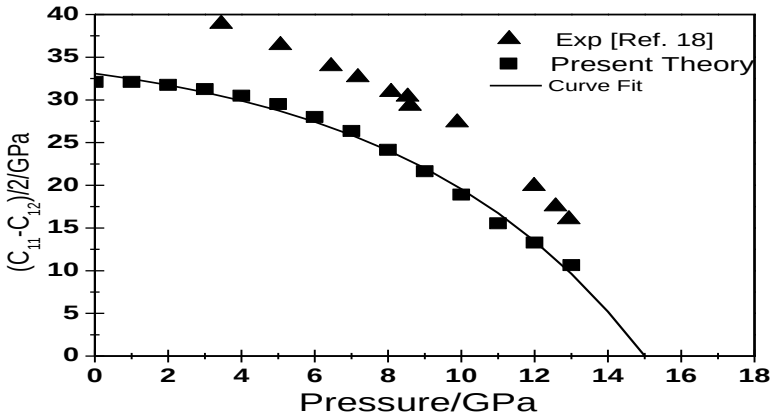

Figure 11: Pressure dependence of shear modulus (C11-C12)/2 of the rutile structure SnO2. The triangle represents the experimental values. Curve fit is the nonlinear curve fitting using the equation, $y = A_1 \exp\left(-x/t_1\right) + y_0$ where A1= -3.8415, t1 = -6.6310, y0=36.9933GPa.

The present report investigated the phonon dispersion curves, zone centre phonon and Raman and IR intensities up to pressure 20 GPa. The ferroelastic transition from the rutile to $CaCl_2$ type structure was confirmed. The soft mode behavior of B_{1g} mode in the rutile structure was observed at transition pressure. We found that the results of the present calculations on phonon dispersion curves and the transition pressure is reproduced and compare very well with the available experimental data in contrast to previous calculations. The rutile to $CaCl_2$ transition involves the softening of shear modulus and Raman active B_{1g} mode with pressure therefore the optimization of structure (lattice constants and atomic coordinates) under symmetry constrains at different pressure is essential for a detailed understating of transition. The Raman and IR intensities plots with pressure show shift in the peaks positions towards the higher frequency side except the Raman active B_{1g} mode which not only shift towards low wavenumber but the intensity also diminishes. Furthermore, our results show that the calculation of the lattice dynamics can be a reliable way to predict transition pressure by monitoring the pressure dependence of phonon frequencies. Finally, the high pressure study or accurate prediction of phase transition in SnO_2 may help in understanding the phase transitions of SiO_2 as this could be involved in some of the seismic anomalies observed in the lower mantle of the earth. Further, our present theoretical calculations reproduce the experimentally determined pressure response of the vibrational modes of rutile SnO_2 and hence give confidence for the accurate predictive power of first principles calculations.

3. Vibrational and Elastic Properties as a pointer to Stishovite to $CaCl_2$ ferroelastic phase transition in RuO_2

3.1. Structural Properties

At a first step the structural optimization of rutile and $CaCl_2$ type RuO_2 has been performed under the minimum condition of total energy and the forces acting on atoms; for each pressure needed in response function calculations. As a result, we calculated the equilibrium structural and internal parameters. The lattice constants and internal parameters, obtained at equilibrium conditions, agree well with the available experimental and previously reported theoretical. In order to reveal behavior and their role played in the stability of structures and phase transformation from rutile to $CaCl_2$ type RuO_2, the total energies for rutile RuO_2 and $CaCl_2$ structures as a function of normalize lattice parameters, unit cell volume and ratio of normalized lattice parameters, are calculated.. The ab-initio calculations are carried out at high pressures up to 14 GPa enforcing its zero pressure symmetry throughout the simulations. In this interval, the lattices parameters, the unit cell ratio c/a and volume (V) change linearly even beyond the phase transition pressure for rutile phase. The calculated quantities reveal the same behaviour as observed in the experimental measurements for one of the isostructure of SnO_2 rutile phase. However, for the $CaCl_2$ type of RuO_2 case the structural lattice parameters a/a_0, b/b_0, c/c_0 and V/V_0 vary linearly up to 14 GPa while (bb_0/aa_0) and (a_0c/ac_0) at 8 GPa show the abrupt change (anomaly) near the phase transition pressure. This clearly indicates that the $CaCl_2$ phase changes from the $CaCl_2$ phase to rutile phase during the reverse heating cycle observed in recent experiment at 1000K and 7.3 GPa to 300K and 5 GPa. The optimized unit cell of RuO_2 is used further for the calculations of electronic band-structure and phonons properties at several pressures.

3.2 Vibrational Properties

To understand the changes that occur in the vibrational spectrum of RuO_2 with pressure, we have performed the full phonon calculations at several pressures up to 14 GPa and 18 GPa for rutile and high pressure $CaCl_2$ phase respectively, using first principles calculations within the DFT formulation. It has been reported in literature that the frequency of B_{1g} Raman mode decreases with decreasing temperature or increasing pressure contrary to the typical behavior normally observed for other Raman active phonon modes of rutile dioxides. This softening of the B_{1g} Raman mode indicates a structural instability, which is a precursor of phase transition. The $CaCl_2$ optic modes have the irreducible representations:

$$2_{Ag} + 2_{B1g} + B_{2g} + B_{3g} + 2B_{1u} + 4B_{2u} + 4B_3$$

Where symbols g, u, E and A and B represent Raman active, infrared active, degenerate modes and non-degenerate modes respectively. Raman active modes are indicated by superscript R, infrared active by IR and unmarked modes are silent. All Raman modes of both phases involve no displacement of Ru ions as they occupy the centrosymmetry positions whereas all IR modes involve Ru sublattice vibrations against oxygens. Three modes with zero frequencies were assigned to the acoustic modes. The present value of B_{1g} mode 125 cm^{-1} is close to the one obtained by in contrast to the who obtained same as 165 cm^{-1}. It is noteworthy that the found a higher transition temperature.

The evolution of phonon modes with pressure is presented shows that the frequency of all optic phonon modes except Raman active B_{1g} mode of the rutile RuO_2 increases with pressure, whereas frequency of all optic phonon modes in $CaCl_2$ phase of RuO_2, increases with pressure. It can be seen clearly that the B_{1g} Raman active optical phonon mode diminishes rapidly with pressure and intercept to zero frequency occurs beyond the phase transition pressure. It is well established from landau theory that the behaviour of the normalized volume and lattice parameters mentioned above are all characteristics of a transition that is second order or very close to second order. A second order transition occurs from a rutile to $CaCl_2$ type structure; i.e. $P4_2/mnm$ (D_{4h}) to Pnnm (D_{2h}), where softening of B_{1g} Raman active phonon mode plays an important role and correspond to the librations of the RuO_6 octahedra about the Z- axis. Thus B_{1g} Raman active phonon mode directly transforms as x^2-y^2 due to spontaneous strain. The transformation recognized as ferroelastic and the spontaneous strain is the primary order parameter. This spontaneous strain can be represented with the relation of direct order parameter and phase transition pressure. The softening of B_{1g} Raman active phonon mode indicates structural instability, which is the precursor of phase transition. In this case the driving force is the B_{1g} Raman active optical phonon mode and the transition occurred before B_{1g} approaches to zero at applied high pressures.

To investigate the softening in the B_{1g} Raman active phonon mode more clearly and confirm the phase transition, we plot the pressure variation of the square of the frequency of B_{1g} phonon mode. Our work reveals that the square of B_{1g} Raman mode softens completely and approaches to zero at 14.27 GPa. This reveals that rutile structure is not stable beyond this pressure. The bilinear coupling of the order parameter to the elastic strain renormalizes the phase transition pressure from rutile to $CaCl_2$ phase. The coupling of elastic strain leads to an acoustic soft mode that approaches zero before the order parameter Q, itself does. Therefore, Raman active B_{1g} phonon mode exhibits a minimum at the phase transition, but does not approach zero. The phase transition pressure obtained from this by fitting our data to least square fit is 8.0 GPa agreeing quite well with the available data]. We have also tried to analyse the rotation angle O-Ru-O bond with respect to diagonal directions in octahedra for

the onset of the rutile to $CaCl_2$ phase transition in RuO_2. The analysis suggests that the rotation angle requires a critical angle of $\cong 8^0$, for transition from rutile to high pressure $CaCl_2$ phase. The trepresentations of the energy eigenvector B_{1g} (corresponding to O-Ru-O bond) in the rutile structure shows that the *O* atoms rotate perpendicular to the [001] direction, while *Ru* atoms remain fixed, resulting in an orthorhombic distortion of the tetragonal unit cell.

In order to investigate the coupling of B_{1g} Raman active mode to the order parameter which is directly related to the responsible transverse acoustic mode for the transition in rutile RuO_2, we have calculated the second order elastic constants at high pressures by slightly distorting the lattice under an orthorhombic strain and reoptimizing the ionic positions in the strained lattice. The elastic constants C_{44} and C_{66} show almost a linear behaviour with pressure. The soft acoustic mode $C_{sm}=(C_{11}-C_{12})/2$ gives direct bilinear coupling with the bare elastic constants. The shear modulus C_{sm} approaches zero at 5.51 GPa implying that this is the transition pressure which suggests a strong coupling between Raman mode and elastic constants and can be attributed to the calculation with ionic relaxations and orthorhombic strains, since without ion relaxation the structure does not access the compression mechanism of lattice, and shear modulus remains high and without altering orthorhombic strain the B_{1g} mode does not soften to zero at the transition.

We also obtained a full phonon dispersion curves at ambient and high pressures for both tetragonal rutile and orthorhombic $CaCl_2$ phases. The present dispersion curves of rutile RuO_2 is in good agreement with previously calculated phonon dispersion curves. However, at 5.0 GPa one branch of the acoustic phonons softens in the vicinity of the Γ (zone centre) point along the Γ-M direction of the Brillouin zone. This mode eventually softens more and becomes unstable at higher pressures. A closer inspection of the phonon dispersion curves reveals that the lattice dynamical instability begins due to the appearance of imaginary frequencies at the pressure of 5 GPa relatively below the pressure of 8 GPa. Figure 6(b) supports the dynamical instability and leads to the second order phase transition from rutile to $CaCl_2$ type phase.

To check the dynamical stability of RuO_2 in high pressure $CaCl_2$ phase, we have also investigated the phonon dispersion relations for $CaCl_2$ type RuO_2 at ambient and high pressures. We found that the phonon dispersion curves for $CaCl_2$ type RuO_2 is quite similar of the rutile RuO_2 which is quite obvious as the both structures are closely related. The X-S and S-Y phonon modes clearly reveal mirror symmetry with flat phonon modes. However, at 8 GPa phonon branches in S-Y directions remove the degeneracy and mirror symmetry between S-Y and S-X disappears. Prominent splitting of E_g mode of rutile RuO_2 in B_{2g} and B_{3g} modes of $CaCl_2$ RuO_2 is also clearly visible. This may be attributed to distortion of tetragonal phase and the coupling of the B_{1g} mode with transverse acoustic phonon modes leads to the RuO_6 octahedra rotations and becomes the precursor of phase transition. Our results show that the calculated T_c and λ increases with increasing pressure, while $<\omega_{log}>$ decreases. Also the $<\omega_{log}>$ of the $CaCl_2$-RuO_2 is larger than that of the Rutile-RuO_2. The λ has the largest value near the onset of dynamical stability and then decreases as increasing the pressure and approaches to the phase transition pressure in rutile phase. Over the pressure range investigated, T_c correlates well withλ, indicating the phonon-mediated superconductivity.

4. First principles calculations of structural, mechanical and phase transition of Be compounds

We have also investigated the structural, mechanical, phase transition, electronic band structure, phonon and thermodynamical properties of three beryllium chalcogenides namely BeS, BeSe and BeTe at ambient and high pressure using plane wave pseudopotential method

within localized density approximation under the density functional theory. There is a good agreement in the case of calculated lattice parameters for B3, B8 and B1 phases of these compounds with experimental and other theoretical data.

Our static calculations for beryllium chalcogenides reveal that these compounds follow B3→B8 phase transition. The phase transition pressure comes out to be 64.24 GPa for BeS, 54.16 GPa for BeSe and 39.9 GPa for BeTe respectively. The electronic band structure and density of states calculations show that the beryllium chalcogenides at ambient condition is semiconducting in nature. In particular, there is a significant hybridization "s" and "p" orbitals of chalcogen atoms and "s" orbitals of Be atom illuminating the mixture of covalent and ionic bonding. The phonon dispersion curves of zinc blende beryllium chalcogenides at ambient conditionshow dynamical stable structure due to the real frequency phonon modes throughout the Brillouin Zone. The phonon dispersion curves of these compounds for B8 and B1 structures contain imaginary frequency for phonon modes at ambient condition indicating lattice instability. The lattice instability disappears with application of pressure and structure becomes dynamically stable. The thermodynamical behaviors for three considered beryllium compounds are normal and we do not observe any anomalous behavior.With applied pressure, dielectric constant increases and Born effective charge decreases for beryllium chalcogenides in B3 phase.

List of Publications:

A. *Papers Published in Journals*

1. Vibrational and Elastic Propeties as pointer to Stishovite to CaCl2 ferroelastic phase transition in RuO_2, S.D Gupta and Prafulla K. Jha, Earth and Planatory Science Letters, 401, 31-39 (2014)
2. A first principles study of phase stability, bonding, electronic and lattice dynamical properties of beryllium chalcogenides at high pressure, Shweta Dabhi, Venu Mankad, Prafulla K. Jha, Journal of Alloys and Compounds 617, 905–914 (2014).
3. A comparative study of experimental and theoretical results of conformations of oxovanadium(IV) complexes with 4-acyl pyrazolone ligands using DFT method, Sanjay Parihar, Sanjeev K. Gupta, R.N. Jadeja, Prafulla K. Jha, Spectrochimica Acta Part A: Molecular and Biomolecular Spectroscopy 128, 447–451 (2014).
4. Zeolite-Y entrapped bivalent transition metal complexes as hybrid nanocatalysts: density functional theory investigation and catalytic aspects, Chetan K. Modi, Parthiv M. Trivedi, Jiten A. Chudasama, Haresh D. Nakum, Digvijaysinh K. Parmar, Sanjeev K. Gupta and Prafulla K. Jha, Green Chemistry Letters and Reviews, 7, No. 3, 278–287, 2014.
5. A first principles lattice dynamics and Raman spectra of the ferroelastic rutile to $CaCl_2$ phase transition in SnO_2 at high pressure, Sanjay D. Gupta, Sanjeev K. Gupta, Prafulla K. Jha and N. N. Ovsyuk, J. Raman Spectrosc. 44, 926–933 (2013).
6. Structural, electronic and dynamical stability of heavy metal iron pernitride: a spin polarized first-principles study, Sanjay D. Gupta, Sanjeev K. Gupta, and Prafulla K. Jha, Eur. Phys. J. B, 86: 8, 3-7 (2013).
7. Size and dimension dependent diffusion coefficients of SnO_2 nanoparticles, Purvi A. Bhatt, Arun Pratap, and Prafulla K. Jha, AIP Conf. Proc. 1536, 237, (2013).
8. "Temperature effect on Raman spectroscopic study of the Fe doped $La_{0.67}Sr_{0.33}MnO_3$ prepared using ball milling method, Nidhi M Astik, Prafulla K. Jha and Vasant Sathe Physics of Solid State Physics,611-8 (2019)".

9. Influence of Fe submission on structure and Raman Spectra of $LaSrMnO_3$: Experimental and density functional studies, Nidhi Astik, H. Soni, P. K. Jha and Vasant Sathe Physics B: Condensed Matter, 541, 103-110 (2018).
10. "Structural , morphological, and thermal properties of ball milled Fe doped nanoscale $La_{0.67}Sr_{0.33}MnO_3$", Nidhi Astik, Prafulla K Jha, and Arun Pratap, J. Electron. Mater. 47, 1937-1943 (2018).

B. ***Papers Published in Conference Proceedings***

1. Investigation on Structural, Electrical and Magnetic Propertoes of Mixed (Mg) Ferrite Systems, Nidhi Astik and G.J. Valdha, National Conference on New Trends in Physics and Materials Science, CSA Govt. PG College, Sehore, Bhopal, 25-26 Sept. 2013**.**
2. Investigation on Structural, Electrical and Magnetic Propertoes of Mixed (Cd) Ferrite Systems, Nidhi Astik and P.K. Jha, Int. Conference on Condensed Matter Physics, H.P. University, Shimla, 4-6 Nov. 2014.
3. Synthesis and characteristic of nanocrystalline $La_{0.67}Sr_{0.33}MnO_3$ manganites by solid state reaction route, Nidhi Astik, Swapnilkumar Patil, and Prafulla K Jha, AIP Conference Proceeding 1728, 020467 (2016).

(iii) Has the progress been according to original plan of work and towards achieving the objectives. YES

(iv) Please indicate the difficulties, if any, experienced in implementing the project

NA

v. If project has not been completed, please indicate the approximate time by which it is likely to be completed. A summary of the work done for the period (Anual basis) may be sent to the commission on a separate sheet.

This is final report.

vi. If the project has been completed. Please enclose a summary of the findings of the study. Two bound copies of the final report of work done may also sent to the commission.

It is described in the report.

viii. Any other information which would help in evaluation of work done on the project. At the completion of project the first report should be indicate the output. Suach as

(a) Manpower Trained : One

(b) Ph. Awarded : One (submitted)

(c) Publication of results : Thirteen Papers have been published in reputed journals

(d) Other impact: The work will have good impact on the basic as well as applications of the studied systems. Further, the work will form a good data base for the studied compounds in present study.